

## Chapter 6

# Stabilization of an Endo- $\beta$ -1,3-1,4-Glucanase by Cyclization

Van Lieshout, J.F.T., Pérez Gutiérrez, O.N., Vroom, W., Koutsopoulos, S., Planas, A., De Vos, W.M., Van der Oost, J.

*submitted*

## Abstract

A novel protein-engineering approach has recently been developed on the basis of intein-driven protein splicing. A modification of this process allows for the generation of a covalent linkage between the N-terminus and the C-terminus of a polypeptide chain. This method has been applied to create circular variants of endo- $\beta$ -1,3-1,4-glucanase (LicA) from *Bacillus licheniformis*. Two cyclic variants were selected for further analysis: LicA-C1 has a linking loop of 20 amino acid residues, and LicA-C2 of 14 residues. Both have a higher thermal stability than the linear variant. Upon increasing temperatures, fluorescence spectroscopy as well as differential scanning calorimetry demonstrated that the cyclic enzymes start to unfold significantly later than the linear one. Both cyclic variants show catalytic activities comparable to that of the linear variant. Moreover, whereas the linear glucanase (LicA-L1) has lost half of its activity after 3 minutes at 65 °C, the two cyclic variants have 6-fold (LicA-C1) and 16-fold (LicA-C2) increased half-life times of inactivation. The most stable enzyme is the cyclic variant with the shortest linking loop.

## Introduction

The application of enzymes as biocatalysts in industry has increased considerably over the last few decades [1-3]. Desired features for optimal performance in a bioreactor include high specificity, high activity and high stability. Because natural enzymes have evolved to function optimally in the context of a living cell, it is not likely that such proteins meet all chemical, physical and biological requirements for being perfect biocatalysts in a specific biotechnological application. Limited shelf life and low intrinsic stability of enzymes often are major drawbacks for an enzyme's successful application. Both random and directed mutagenesis strategies have been used to create variants with optimized features, either by improving specificity or activity of stable thermophilic enzymes [4-6], or by increasing stability of labile mesophilic enzymes with desired catalytic features [7, 8]. Intrinsic factors that contribute to thermostability include ionic or hydrophobic interactions, improved subunit interactions, reduced surface area, improved packing, or a combination thereof [9, 10]. To stabilize a protein, these factors have to be introduced by random or directed mutagenesis approaches in the corresponding gene (reviewed by [11]).

A rather poorly explored feature is stabilization of a protein by a covalent cyclization of its backbone structure. Several peptides (or small proteins) have been identified in bacteria, plants and mammals that have a covalently-linked N- and C- terminus [12, 13]. Not only are they more stable at a broad range of chemical and physical conditions, they often also show an increased resistance to proteases [14]. Although details on the biosynthesis of most of these naturally occurring circular proteins are still unknown, several studies have proven that it is possible to engineer a covalent linkage of the N-terminal and C-terminal amino acids of a polypeptide chain, thereby generating a cyclic enzyme. Distinct cyclization strategies have been developed: (i) a chemical approach that applies solid phase synthesis combined with chemical ligation or crosslinking [15, 16], (ii) a biochemical strategy based on intein-driven self-ligation *in vitro* [17, 18], and (iii) a biological

method that is based on the ability of inteins to perform self-splicing *in vivo* (Fig. 6.1) [18-20]. Little is known about the effect of cyclization on protein stability since limited information has been reported in the few previous studies [17-20].

In the present study *in vivo* cyclization has been applied to the endo- $\beta$ -1,3-1,4-glucanase (LicA) from *Bacillus licheniformis* in order to study the effect of covalently linking the N- and C-termini on catalysis and stability. Bacterial 1,3-1,4- $\beta$ -glucanases (or lichenases, EC 3.2.1.73) hydrolyze  $\beta$ -1,4-glycosidic bonds on 3-*O*-substituted glycosyl residues in linear mixed-linked glucans, like barley  $\beta$ -glucan and lichenan, and have been studied extensively over the years (reviewed by Planas 2000 [21]). These enzymes are classified in family 16 of glycoside hydrolases [22] and have a monomeric jelly-roll  $\beta$ -sandwich structure [23-25] (Fig. 6.2). The monomeric structure of LicA, with the N- and C-termini in close proximity, makes the *in vivo* intein-based method a particularly suitable strategy for this enzyme.

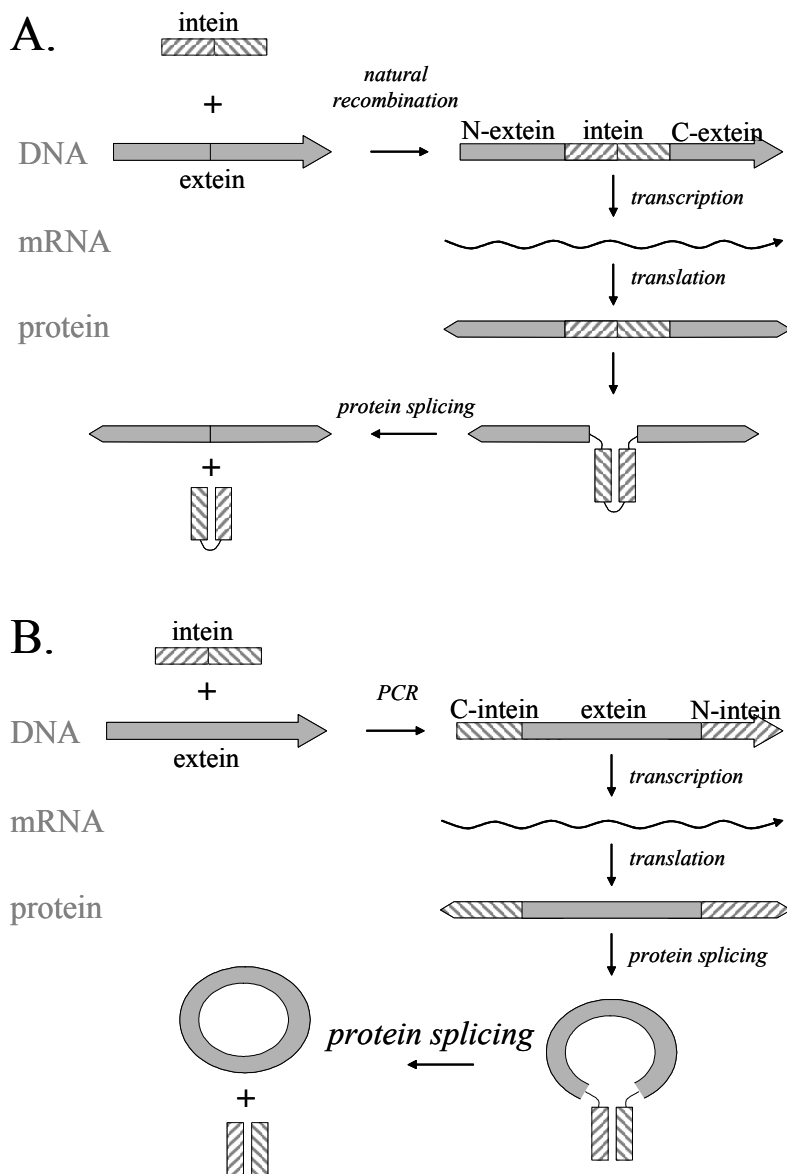


**Figure 6.1.** Inteins in nature and as engineering tool. **(A)** Protein splicing by a natural intein, resulting in ligation of the two extein fragments. **(B)** The engineered split intein domains do fold, interact and form an active intein complex that catalyzes splicing and ligation of the extein fragment as does the aforementioned natural system. The result is a complex of the two intein domains, and the extein domain with a circular peptide backbone.

**Table 6.1.** Primers used in this study

\* s = sense, a = antisense

† sequences are given from 5'-3'

Primer*	primer sequence†	Description	LicA-variant
BG1260 s	GCGCGCCATGGGACATGAGTACATCTATGACAGA	intein C + <i>Nco</i> I-site	C1(a), C1-C6
BG1261 a	GTGGTGGTGGTGGTGGTCCGGTGTGGACGAAAATCATTC	intein C + His-tag	C1(a), C1, C2, C6
BG1262 s	GGACACCACCACCACCACCACCCAAACGGGCGGGTCGTTTTATGAAC	glucanase + His-tag	C1(a), C1, C2, C6
BG1263 a	CCCCGTTCCCTCGTGGTACTAGTCTTTTTGTGTAAACGCACCCCAATG	glucanase + thrombin-site	C1(a), C1, C5
BG1264 s	CTAGTACCACGAGGAACCCGGGTGCATAGACGGAAAGGCCAAG	intein N + thrombin-site	C1(a), C1, C5
BG1265 a	GCGCGCTCGAGCTTAAACATGTGAGTGGTATTTATC	intein N + <i>Xho</i> I-site	C1(a)
BG1306 s	GCGCGCCATGGGGCAAAACGGGCGGGTCGTTTT	glucanase + <i>Nco</i> I-site + $\Delta$ signalsequence + SA $\rightarrow$ MG	L1
BG1307 a	GCGCGCTCGAGTCTTTTTGTGTAAACGCACCCA	glucanase + <i>Xho</i> I-site + $\Delta$ stopcodon	L1
BG1351 s	GGACACCACCACCACCACCACCCGGTCTGTTTTATGAACCCGTTCAAC	as BG1262 + $\Delta$ QTG	C3, C4, C5
BG1352 a	TGGCCTTTCCGTCTATGCACCCTGTGTAAACGCACCCCAATGTAATGAG	as BG1263 + $\Delta$ thrombin-site + $\Delta$ KR	C3, C6
BG1353 s	CTCATTACATTTGGGTGCGTTACACAGGGTGCATAGACGGAAAGGCCA	as BG1264 + $\Delta$ thrombin-site + $\Delta$ KR	C3, C6
BG1354 a	GCGCGCTCGAGTTACTTAAACATGTGAGTGGTATTTATCAAA	as BG1265 + stopcodon	C1-C6
BG1429 a	TCTATGCACCCCTCTTTTTGTGTAAACGCACCCCAATG	as BG1263 + $\Delta$ thrombin-site	C2
BG1430 s	GTTACACAAAAAGAGGGTGCATAGACGGAAAGGCC	as BG1264 + $\Delta$ thrombin-site	C2
BG1431 a	CCCCGTTCCCTCGTGGTACTAGTGTGTAAACGCACCCCAATGTAATG	as BG1263 + $\Delta$ KR	C4
BG1432 s	CTAGTACCACGAGGAACCCGGGTGCATAGACGGAAAGGCC	as BG1264 + $\Delta$ KR	C4
Intein-f a	CGAGCCGAGGACGTTCTACGATC	forward sequence primer, annealing to intein	-
Intein-r s	GCTTGTATCTCTCGTACATCTCCTC	reverse sequence primer, annealing to intein	-

## Materials and methods

**Bacterial hosts and vectors** - The T7 expression vector pET24d was obtained from Novagen. *Escherichia coli* XL-1 Blue (Stratagene) was used as an initial host for cloning, while either one of the *E. coli* strains BL21(DE3) or JM109 (DE3) (Stratagene) was used as expression host for the pET-derivatives. *E. coli* was grown in TY medium [26] in a rotary shaker at 37°C. Kanamycin was added to a final concentration of 30  $\mu$ g/ml.

**Cloning and expression** - The gene coding for *Bacillus licheniformis* 1,3-1,4- $\beta$ -glucanase previously cloned in the pUC119-derived pD6-2 [27] was used as a template for PCR amplification. For expression of the linear enzyme without the signal sequence the gene was subcloned in pET24d using primers BG1306 and BG1307 (Table 6.1), introducing a C-terminal His-tag, resulting in pWUR146.

*P. furiosus* genomic DNA was isolated as described previously [26] and used as template in PCR reactions to amplify the intein PI-*PfuI* [20, 28]. In a first series of PCR reactions the two parts of the intein and the glucanase gene were amplified separately (Fig. 6.3A). In PCR-2, an overlap extension PCR [29], the three overlapping fragments were fused, and the full-length hybrid molecule was amplified using the flanking primers BG1260 and BG1265/1354 (2.1 kb; Fig. 6.3A). The 2.1 kb PCR product was then ligated into pET24d at the *NcoI* and *XhoI* restriction sites, and transformed to *E. coli* XL1-Blue. Sequence analysis of this construct (and of all variant constructs described below, generated with a similar approach using variant primers (Table 6.1)) was done by the dideoxynucleotide chain termination method with a Li-Cor automatic sequencing system (model 4000L). Two sets of sense/antisense sequence primers were used that anneal either to the promoter and terminator sequence of the pET24d vector, or to the sequences of the two parts of the intein flanking the glucanase gene (Intein-f and Intein-r in Table 6.1).

**Overexpression of the gene and purification of recombinant protein** – Both the *licA-L1* gene and the permuted genes were expressed in freshly transformed BL21(DE3) or JM109 (DE3) cells. A 5 ml overnight culture was used to inoculate 500 ml of TY medium containing 30  $\mu$ g/ml kanamycin. When the OD<sub>600</sub> reached 0.5, the cells were induced with 100  $\mu$ M IPTG and subsequently grown at 37 °C for another 4 h. Cells were harvested by centrifugation (10 min, 4000 x g) and resuspended in 50 mM sodium phosphate buffer (pH 7.7) containing 300 mM NaCl and 10 mM imidazole. After addition of lysozyme to 1 mg/ml, the cells were incubated on ice for 30 min before sonication (six times 15 sec). After removal of the cell debris by centrifugation (30 min, 10,000 x g) the glucanase variants containing a Histidine hexa-peptide (His-tag) were further purified from the supernatant using Ni-NTA spin columns according to the provided protocol for native conditions (Qiagen). The active fractions were collected and purified to homogeneity on a Superdex200 column (Amersham Biosciences). Depending on subsequent analysis of the enzyme, elution was performed with either a 50 mM sodium phosphate buffer (pH 7.7) or a 20 mM PIPES buffer (pH 7.0).

**Enzymatic assays** - Standard enzymatic assays were performed at 55°C in 30 mM sodium phosphate buffer (pH 7.0) containing 0.1 mM of CaCl<sub>2</sub> with barley β-glucan (final concentration 0.4 %) as a substrate. The reducing sugars were detected by the dinitrosalicylic acid (DNS) method, with glucose as standard [30, 31]. One unit is defined as the amount of enzyme required to release 1 μmol of reducing sugars per min. Temperature induced inactivation was determined in 50 mM sodium phosphate (pH 7.7) and 1 mM CaCl<sub>2</sub> by heating the purified enzyme (30 μg/ml) in small crimp-sealed vials, submerged in a water bath. During a time series (0-20 h), 20-μl aliquots were tested for remaining activity as described above. All activities were corrected for spontaneous hydrolysis in the absence of enzyme.

**Thrombin digestion** - To linearize the circular proteins containing a thrombin recognition site, incubation with thrombin (Sigma) was performed overnight at 22 °C. A ratio of 1 unit of thrombin was used per 100 μg of protein.

**Fluorescence emission spectroscopy** - For fluorescence experiments proteins were purified with 20 mM PIPES buffer (pH 7.0) as the eluent in the final step on the Superdex200 column. In 10 mm Quartz SUPRASIL precision cells (Hellma), 20 mM PIPES (pH 7.0) was mixed with the protein solution to a final concentration of 15 μg/ml with a final volume of 3.0 ml. When indicated, 1.0 mM CaCl<sub>2</sub> or 1.0 mM EDTA was added. All solutions were degassed prior to use. The fluorescence emission was measured in the temperature range 30 – 95°C, and with a scan rate of 0.5 °C/min by a Varian Cary Eclipse spectrophotometer. Emission spectra were recorded in the range 300 – 400 nm upon excitation of the tryptophans at 295 nm, with the excitation and emission slit widths set at 10 nm, and the photomultiplier at 610 V. All spectra were corrected for the background emission peak of water. The emission spectra of samples containing 1 mM of either CaCl<sub>2</sub> or EDTA were corrected using buffer baselines acquired at the same conditions.

**Differential Scanning Calorimetry** – Temperature-controlled calorimetric studies of 0.3 mg/ml LicA-C1 were carried out in a VP-DSC calorimeter (MicroCal Inc., Northampton, MA) using as reference the respective buffer solution. All samples were degassed for 15 min prior to loading the cells and the enzyme solution was kept under 1.5 bar pressure to avoid boiling of the sample. The temperature increased with a heat rate of 0.5 °C/min.

## Results and Discussion

Protein stability can be described as the Gibbs free-energy of folding ( $\Delta G$ ), i.e. the difference in free energy between the protein's denatured and native state. The actual net free energy difference is the sum of a large number of stabilizing and destabilizing interactions. This difference is usually very small, typically 5-17 kcal/mol, which is comparable to the energy of only a few hydrophobic interactions, ion pairs, or hydrogen bonds (reviewed by [11]). According to Gibbs' equation ( $\Delta G =$

$\Delta H - T.\Delta S$ ), protein stability ( $\Delta G$ ) can be increased either by increasing the enthalpy change ( $\Delta H$ ) or by decreasing the entropy difference ( $\Delta S$ ). Several examples have been described of “entropic stabilization” (rigidification), i.e. mutations that result in increased  $\Delta G$  because of a decreased  $\Delta S$  (lowering the entropy of the denatured state). Such engineering of protein stability includes the engineering of a more rigid protein backbone by specific substitutions (e.g. Gly > Ala in an  $\alpha$ -helix, or Xxx > Pro in a  $\beta$ -turn), or by the introduction of disulfide bridges [11]. An alternative approach to reach entropic stabilization is described in the present study: the covalent linkage of the polypeptide’s N- and C-termini. Apart from enhanced rigidity, such a cyclic polypeptide would also be resistant towards exo-proteases.

The goal of the present study was to introduce a covalent link between N- and C-terminus of an active enzyme, and subsequently analyze potential stabilization of the generated circular backbone structure. The three-dimensional structure of the *Bacillus licheniformis* 1,3-1,4- $\beta$ -glucanase (LicA) [24] indicates that this approach could be feasible since the termini of this enzyme are in close proximity, as they reside on adjacent anti-parallel beta strands (Fig. 6.2). Hence, this enzyme was selected for further engineering experiments.

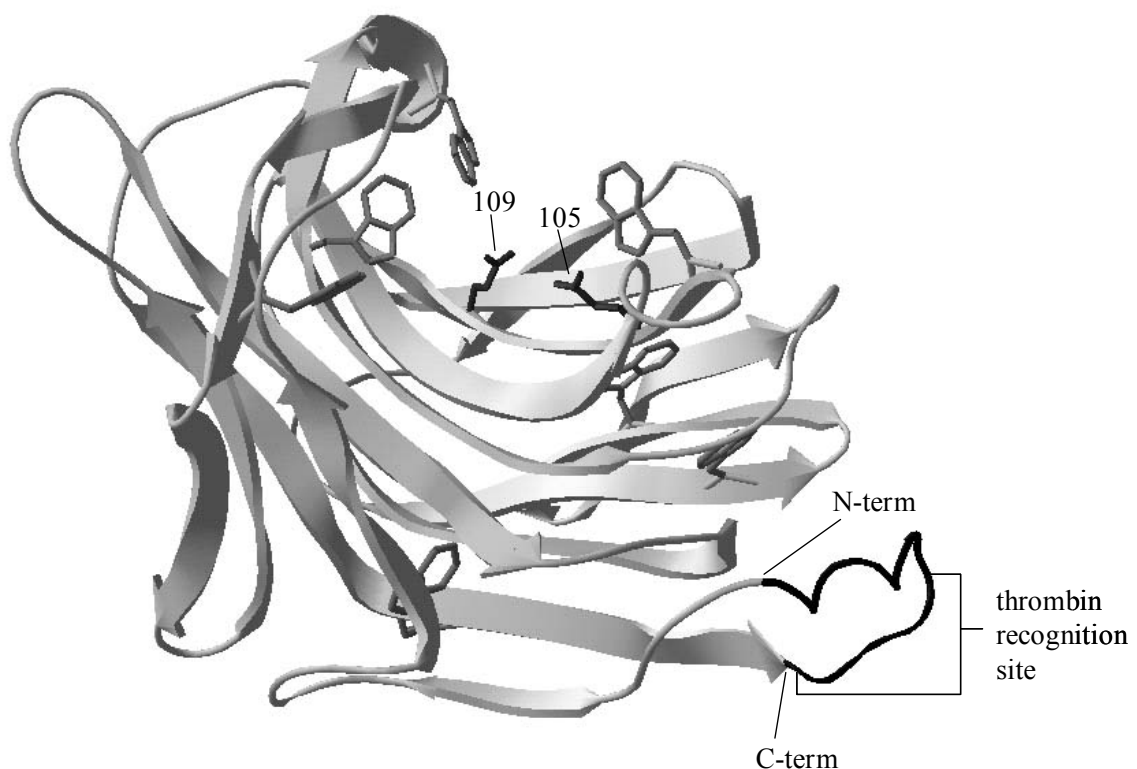
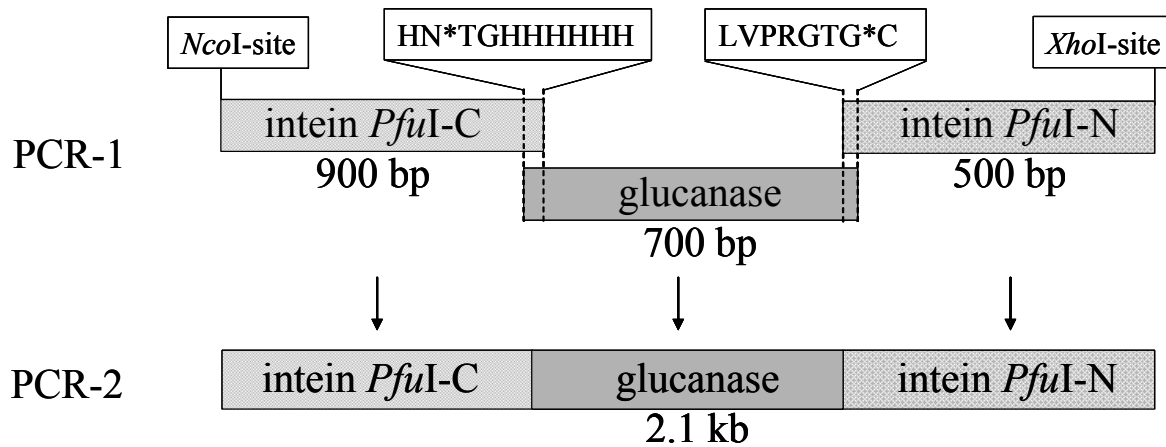


**Figure 6.2.** Circular LicA structural model. The model shown is one possible structure of construct LicA-C1. 15 extra residues were added to the x-ray structure (Protein Data Bank code 1GBG) and manually turned to form a closed peptide backbone with the program Swiss-PdbViewer. The linking loop is shown as a black coil. The original N- and C-terminal locations (Gln-1 and Arg-214 respectively) are indicated, as well as the thrombin recognition site. The two catalytic residues (Glu-105 and Glu-109; numbering according to 3D-structure in Protein Data Bank) are displayed in black. Tryptophan residues are depicted in dark grey.

### A. PCR design of circular LicA



### B. Linear LicA-construct

	[ C-term ]	[ N-term ]	length loop	activity (U/mg)
L1	: <u>...WVRYTKRLEHHHHHH</u>	<u>MGQTGGSFYE...</u>	-	2.7

### C. Circular LicA-constructs

	["C-term"]	*	["N-term"]	length loop	activity (U/mg)
C1	: <u>...WVRYTKRLVPRGTG*</u>	TGHHHHHH	<u>QTGGSFYE...</u>	20	4.9
C1a	: <u>...WVRYTKRLVPRGTG*</u>	TGHHHHHH	<u>QTGGSFYE...</u>	20	4.7
C2	: <u>...WVRYTKR</u>	-----G*	TGHHHHHH	14	7.7
C3	: <u>...WVRYT</u>	-----G*	TGHHHHHH	9	0.0
C4	: <u>...WVRYT</u>	--LVPRGTG*	TGHHHHHH	15	0.0
C5	: <u>...WVRYTKRLVPRGTG*</u>	TGHHHHHH	---	17	7.9
C6	: <u>...WVRYT</u>	-----G*	TGHHHHHH	12	0.0

linking loop

**Figure 6.3.** Circular constructs made in this study. (A) Schematic representation of the PCR-based engineering of the constructs used for the intein-based circularization of LicA; for details see text; *NcoI* and *XhoI* are the introduced restriction sites. The amino acid sequence of the overlap of the PCR-1 fragments is shown. \* indicates the connection point of the sequence of the intein and the glucanase gene; (B/C) Amino acid sequences of the N- and C-terminal regions of (B) linear and (C) circular variants of LicA. The extein sequences, corresponding to the wild-type sequence, are underlined; note that in all constructs the signal sequence has been deleted, resulting in intracellular production of the corresponding proteins. The length of the various loops is indicated, as well as the activity of the purified proteins (U/mg). LicA-C1 and LicA-C1a are identical, but the precursor protein of LicA-C1a has a His-tag at the N-terminal part of the intein, in contrast to that of LicA-C1 (see text). \* indicates the connection point of the N- and C-terminal sequence.



To produce a circular enzyme we used a self-splicing intein to ligate protein backbones. The intein PI-*PfuI* from *Pyrococcus furiosus* has recently been demonstrated to perform this cyclization in *E. coli in vivo* [20], and has therefore been selected for the present study. In a two-step PCR reaction we connected the C-terminal part of the intein (residues 161-454) to the N-terminus of the 1,3-1,4- $\beta$ -glucanase, and the N-terminal part (residues 1-160) to the C-terminus of the 1,3-1,4- $\beta$ -glucanase (Fig. 6.3A). After cloning in pET24d, this resulted in a chimeric gene of 2058 basepairs coding for a precursor protein with a total length of 686 amino acids (79.4 kDa). At the same time, a His-tag was introduced at the N-terminus of the glucanase to facilitate purification. Furthermore, the connecting loop contained a thrombin recognition site (LVPRGT) to enable subsequent linearization by thrombin cleavage. After processing, the cyclic protein LicA-C1 has a length of 229 amino acids (Fig. 6.3C), whereas the linear LicA-L1 consists of 224 amino acids (Fig. 6.3B).

The glucanase gene, without the signal sequence but with His-tag (Fig. 6.3B), was expressed in *E. coli* BL21(DE3) cytoplasm as a soluble protein (LicA-L1). After purification LicA-L1 has a specific activity (2.7 U/mg), comparable to that of the wild-type LicA, expressed with its signal sequence but without His-tag, the excreted mature product of which was purified from the *E. coli* medium (A. Planas, personal communication). This indicates that both the loss of the signal peptide (29 amino acids), and the addition of six C-terminal histidines (Fig. 6.3B), does not have a significant effect on the specific activity of the 1,3-1,4- $\beta$ -glucanase.

Next, cyclic enzymes LicA-C1 and LicA-C1a (Fig. 6.4) were expressed as soluble proteins in *E. coli* cells. Construct LicA-C1 generates, upon *in vivo* processing, a circular glucanase with the His-tag and the thrombin cleavage site in the linking loop that connects the N- and C-termini (Fig. 6.3C). On the other hand, LicA-C1a is a control construct that will produce the same cyclic  $\beta$ -glucanase, but has a second His-tag at the N-terminal part of the intein. Cell-free extracts of *E. coli* BL21(DE3) cells overproducing either LicA-C1 or LicA-C1a showed three prominent additional bands on a SDS-gel, with sizes of 35, 27 and 19 kDa (Fig. 6.4). After application of the LicA-C1a cell-free extract on a Ni-NTA column, the proteins corresponding to these three bands were separated from the *E. coli* proteins (Fig. 6.4). The sizes corresponded to the expected molecular weights of the glucanase and of the C- and N-terminal parts of the intein. This indicates that the splicing reaction has taken place in the cells, leading to three separate polypeptide-fragments. Moreover, the co-purification on the Ni-NTA column shows that the C-terminal part of the intein, lacking a histidine tag, is associated with its N-terminal part, which is necessary for the splicing reaction to take place. A similar phenomenon was observed by Iwai et al. [20], however, they also found the presence of an unprocessed 80 kDa product. The absence of such an unprocessed form in our system indicates the efficiency of the present approach.

In the case of construct LicA-C1, the intein fragments were not affinity-purified on the Ni-NTA column (Fig. 6.4) because the N-terminal intein fragment does not contain a His-tag. In all other variant constructs (see below), this His-tag at the N-terminal intein was omitted as well, resulting in the presence of only a single His-tag, which is located in the linking loop of the circular glucanase, like in LicA-C1, allowing for a convenient 1-step purification of the circular enzymes. Thrombin was added to the purified spliced LicA-C1 protein and incubated overnight. SDS-PAGE analysis (Fig. 6.4) showed a different migration behavior between the thrombin diges-

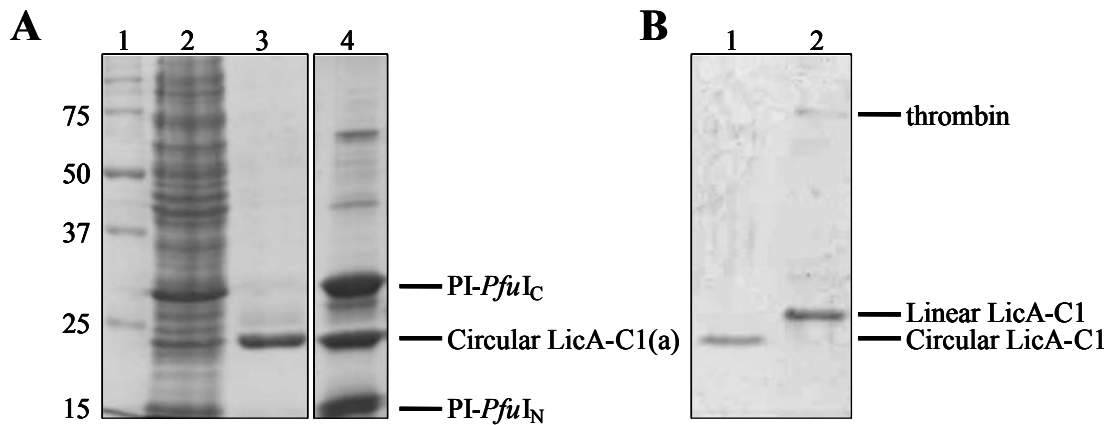


**Figure 6.4.** SDS-PAGE analysis of expressed and purified circular and linearized LicA-C1. **(A)** Lane 1, molecular weight marker, with corresponding sizes shown on the left in kDa. Lane 2, cell free extract of *E. coli* BL21(DE3) expressing construct 1. Lane 3, circular LicA-C1 after purification on a NI-NTA column. Lane 4, circular LicA-C1a after purification on a NI-NTA column. PI-PfuI<sub>C</sub> and PI-PfuI<sub>N</sub> denote the C- and N-terminal part respectively of the intein, that are visible in lane 2 and 4. **(B)** LicA-C1 after purification on Superdex200, before (Lane 1) and after (Lane 2), treatment with thrombin.

ted sample and the untreated protein. The non-digested LicA-C1 protein migrates faster (Fig. 6.4), as would have been expected for a circular form because of its slightly different denatured conformation. This phenomenon has been reported before with circular and linearized polypeptides [17, 19, 20].

The cell-free extracts containing the circular protein LicA-C1 showed hydrolytic activity on barley- $\beta$ -glucan, reflecting its proper folding. After purification, the specific activity of the circular enzyme is comparable to that of the linear one, apparently slightly more active (Fig. 6.3). Fluorescence spectroscopy after excitation at 295 nm demonstrated a similar emission spectrum of the linear LicA-L1 and the circular LicA-C1 (not shown), also suggesting correct folding of the protein. The optimal temperature for hydrolytic activity for the spliced protein was determined to be 56 °C, which is in the same range as the 55°C optimum of the wild-type enzyme [32].

From these results we conclude that endo-1,3-1,4- $\beta$ -glucanase was expressed, excised and ligated successfully to acquire its designed circular backbone structure. Moreover, the comparable activities of the circular enzyme variant LicA-C1 and the linear LicA-L1 indicate that the introduced junction and loop do not result in inactivation of the enzyme, indicating that the enzyme's functionality has not been affected by the generated covalent link. Earlier studies showed that circular permutations in the compact jellyroll domain of the *Bacillus* glucanase is tolerated without severe change of enzymatic activity or tertiary structure [33, 34]. In the latter studies, it was concluded that the novel peptide bond linking the original N- and C-termini, without adding extra residues, apparently did not introduce strain into the molecule. However, in those studies new N- and C-termini were introduced in another loop of the glucanase structure, and as such there was still an open chain (linear) structure, which might enable release of strain. In our study, a covalently-closed circular polypeptide chain is generated in which a high specific activity indicates that no severe strain is introduced.

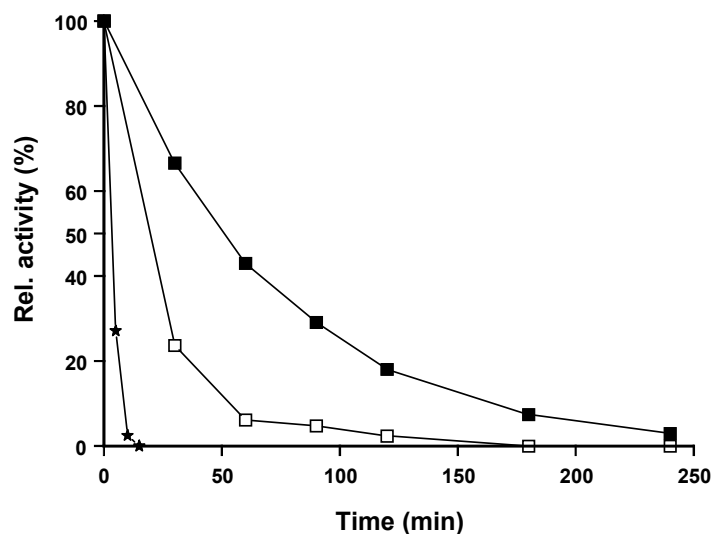


**Figure 6.5.** Temperature induced inactivation. Residual activity of linear LicA-L1 (asterisks), circular LicA-C1 (open squares) and circular LicA-C2 (closed squares), when incubated at 65 °C at a concentration of 30  $\mu$ g/ml in a 50 mM sodium phosphate buffer (pH 7.7) containing 1 mM  $\text{CaCl}_2$ . Activity of each sample is expressed relative to the sample measured at  $t=0$ , taken as 100%.

The effect of the ligated backbone on thermostability was investigated by comparing the thermal inactivation of LicA-C1 with that of LicA-L1. Incubation at 65 °C caused the linear enzyme to inactivate very rapidly ( $t_{1/2} = 3$  min; Fig. 6.5). Complete inactivation occurred within 15 min. The cyclic LicA-C1, however, still retained half of its initial activity after 20 min (Fig. 6.5), a 6-fold increase as compared to the linear LicA-L1.

Temperature-induced unfolding was monitored by fluorescence spectroscopy to determine the transition midpoint of the linear enzyme in comparison with its cyclic derivative, as an alternative means to study the effect of cyclization on protein stability. A titration of a protein solution with a chemical or physical stress factor (e.g. temperature gradient) generally results in a transient rearrangement of the polypeptide structure, and consequently in a transient decrease of the tryptophan fluorescence emission. The LicA enzyme contains 8 tryptophan residues that are randomly distributed over the protein backbone (Fig. 6.2), which were used as intrinsic fluorophores for fluorescence emission studies upon excitation at 295 nm. The fluorescence intensities of the linear and the circular LicA were monitored at 350 nm as a function of temperature (Fig. 6.6). The intensities measured at different wavelengths (360 and 375 nm) gave similar transition temperatures (not shown).

First the effect of calcium was examined. While addition of EDTA caused the linear enzyme to melt at 61.8 °C, the presence of calcium resulted in a melting temperature of 64.5 °C. This confirmed the stabilizing effect of calcium for endo-1,3-1,4- $\beta$ -glucanase as reported before [35, 36], and calcium was added in all further experiments. In the presence of calcium, the circular LicA-C1 showed a melting temperature of 67.7, an increase of 3 °C as compared to the linear LicA-L1 (Fig. 6.6); a destabilizing effect of EDTA as described for the linear enzyme, was also observed with the circular variants (results not shown). The apparent melting temperatures obtained for linear and circular enzymes match very well with the trend observed in the above mentioned in-

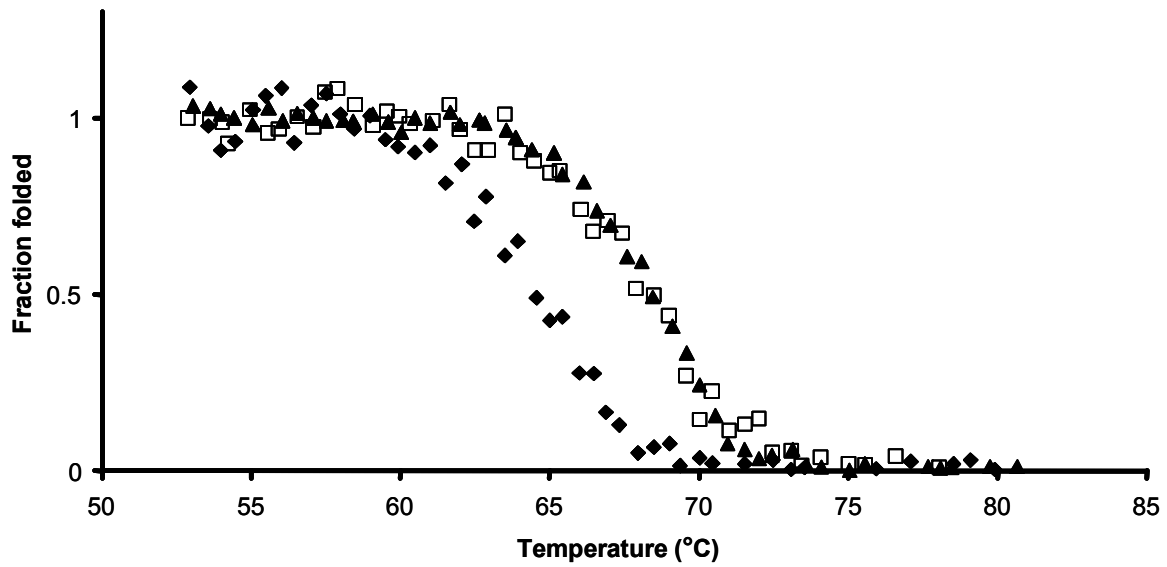


**Figure 6.6.** Temperature induced unfolding. Fraction of folded linear LicA-L1 (closed clubs), circular LicA-C1 (open squares) and circular LicA-C2 (closed triangles), upon increasing temperature. Fraction was calculated by normalizing the emission data at 350 nm obtained by thermal denaturation fluorescence spectroscopy.

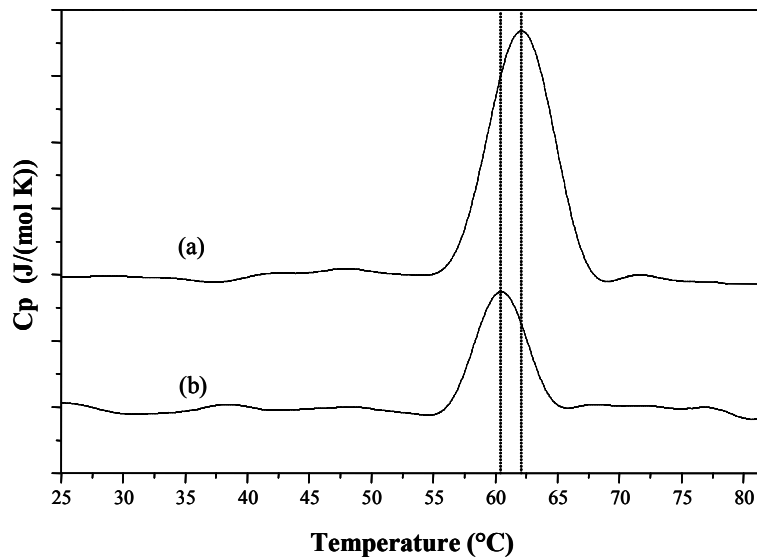


**Figure 6.7.** Temperature induced unfolding. Differential scanning thermograms of (A) LicA-C1 and (B) linearized LicA-C1 in the absence of  $\text{Ca}^{2+}$  at pH 7.00 at a protein concentration of 0.3 mg/ml. Graphs were vertically shifted for comparison. Vertical dotted lines emphasize the shift of the denaturation temperature.

activation experiment at 65 °C (Fig. 6.5). While the linear enzyme is beyond its melting temperature at this condition and thus starts to inactivate rapidly, the circular variant is only at the early stage of unfolding, resulting in a much slower inactivation process.

DSC studies of circular and linearized (circular variant after treatment with thrombin) LicA-C1 in 50 mM sodium phosphate buffer (pH 7.7), revealed a single denaturation transition peak. The denaturation temperature,  $T_d$ , was found to be 60.0 °C and 61.7 °C for the linearized and the circular LicA-C1, respectively (Fig. 6.7). These denaturation temperatures are in good agreement with the transition temperatures observed from monitoring the fluorescence intensity under the same conditions. Varying the scanning rate between 0.25 and 1.5 °C/min did not affect the  $T_d$  or the shape of the endothermal peak and the enthalpy associated with the transition (not shown). However, after cooling the samples to room temperature subsequent heating up did not reveal a denaturation peak; this indicates irreversible unfolding that prevents the calculation of changes in  $\Delta S$  and  $\Delta H$ . However, from the area of the transition peak, the calorimetrically-determined enthalpy associated with the denaturation of the circular enzyme was estimated to be two-fold higher than that calculated for the denaturation of the linearized enzyme (not shown). The enthalpy of denaturation is a measure of the intramolecular bonds, which maintain the active protein conformation. This strongly suggests that the backbone cyclization increases the internal stability of LicA-C1.

To investigate the effect of the introduced loop, a series of constructs with different lengths and composition were designed. Shorter loops were constructed either by deletion of three N-terminal residues (QTG), two C-terminal residues (KR), the thrombin recognition site (LVPRGT), or a combination thereof, resulting in linking loops consisting of 9 - 20 amino acid residues (Fig. 6.3C). The six histidine residues were always maintained to facilitate purification. Based on SDS-PAGE analysis of Ni-NTA purified CFEs of the complete series of clones, it is concluded that not all variants were produced as soluble proteins; the cases where no protein band was detectable corresponded to the ones in which no activity was measured (LicA-C3, LicA-C4 and LicA-C6) (Fig. 6.3C). The constructs for which proteins of the expected size were detected (not shown), were purified and activity was analyzed: LicA-C1, LicA-C2 and LicA-C5. The two variants with the shortest loop (LicA-C3 and LicA-C6) are inactive, whereas the ones with a longer loop (LicA-C1 and LicA-C5) show hydrolytic activity (Fig. 6.3C). On the other hand, the medium-sized loops result in both an active (LicA-C2) and an inactive (LicA-C4) cyclic variant, at least indicating that length is not the only factor affecting catalytic function and/or correct processing. Moreover, it can not be ruled out that the C-terminal residues (RK) are important; a mutant with only this deletion has not been included. Removal of the N-terminal QTG or the thrombin recognition site has hardly any effect. Overall, it is concluded that both the size of the loop and the nature of amino acid residues in the region of the original C-terminus, determines the efficiency of intein processing, which is required to generate active circular endo-1,3-1,4- $\beta$ -glucanase.

The variant with the shortest loop that was still active, LicA-C2, was compared with the long loop variant, LicA-C1, with respect to temperature optimum and stability. Like variant LicA-C1, also LicA-C2 had an optimal temperature of 55 °C, identical to the linear LicA-L1 (not shown). Both cyclic variants are more stable than the linear enzyme. Fluorescence spectroscopy showed that

variant LicA-C2 unfolds in the same temperature range as variant LicA-C1 (Melting temperature of 68.2 °C, Fig. 6.6). As discussed earlier, LicA-C1 inactivated 6-fold slower than LicA-L1 upon incubation at 65 °C, yet LicA-C2 showed an inactivation half-life time of 50 min at this temperature: more than a 16-fold increase as compared to the linear enzyme (Fig. 6.5). The difference in stability between the two cyclic variants is significant. LicA-C2 differs from LicA-C1 by the deletion of 6 amino acid residues, the thrombin recognition site, in the loop (Fig. 6.3C). The shorter loop of LicA-C2 might result in a more stable protein because it is more compact, whereas the longer loop of LicA-C1 might be more flexible, what makes the protein more susceptible to unfolding at increasing temperatures. Furthermore, solving the three-dimensional structures of LicA-C1 and LicA-C2 would be required to reveal interactions between residues in the loop and other residues that might contribute to stability of the cyclic enzymes.

In summary, the endo-1,3-1,4- $\beta$ -glucanase from *Bacillus licheniformis* has successfully been circularized by using the cyclization approach based on circular permutation of a precursor protein flanked by two intein domains. The circular variants showed catalytic properties comparable to the original linear enzyme, but were significantly more stable. Although the design of the connecting loop will differ per protein, we conclude that cyclization may be an effective tool to moderately stabilize polypeptides.

## Acknowledgments

This research was supported by the Technology Foundation (STW), applied science division of NWO and the technology programme of the ministry of Economic Affairs. O. P. received a fellowship of the VLAG graduate school (Wageningen University).

## References

1. van Beilen, J. B. & Li, Z. (2002) Enzyme technology: an overview, *Curr. Opin. Biotechnol.* **13**, 338-344.
2. Kirk, O., Borchert, T. V. & Fuglsang, C. C. (2002) Industrial enzyme applications, *Curr. Opin. Biotechnol.* **13**, 345-351.
3. Schmid, A., Dordick, J. S., Hauer, B., Kiener, A., Wubbolts, M. & Witholt, B. (2001) Industrial biocatalysis today and tomorrow, *Nature.* **409**, 258-268.
4. Lebbink, J. H., Kaper, T., Bron, P., van der Oost, J. & de Vos, W. M. (2000) Improving low-temperature catalysis in the hyperthermostable *Pyrococcus furiosus* beta-glucosidase CelB by directed evolution, *Biochemistry.* **39**, 3656-3665.
5. Kaper, T., Lebbink, J. H., Pouwels, J., Kopp, J., Schulz, G. E., van der Oost, J. & de Vos, W. M. (2000) Comparative structural analysis and substrate specificity engineering of the hyperthermostable beta-glucosidase CelB from *Pyrococcus furiosus*, *Biochemistry.* **39**, 4963-4970.
6. Kaper, T., Brouns, S. J., Geerling, A. C., De Vos, W. M. & Van der Oost, J. (2002) DNA family shuffling of hyperthermostable beta-glycosidases, *Biochem. J.* **368**, 461-470.
7. Machius, M., Declerck, N., Huber, R. & Wiegand, G. (2003) Kinetic stabilization of *Bacillus licheniformis* alpha-amylase through introduction of hydrophobic residues at the surface, *J. Biol. Chem.* **278**, 11546-11553.

8. **Van den Burg, B., Vriend, G., Veltman, O. R., Venema, G. & Eijsink, V. G.** (1998) Engineering an enzyme to resist boiling, *Proc. Natl. Acad. Sci. U S A.* **95**, 2056-2060.
9. **Yip, K. S., Britton, K. L., Stillman, T. J., Lebbink, J., de Vos, W. M., Robb, F. T., Vetriani, C., Maeder, D. & Rice, D. W.** (1998) Insights into the molecular basis of thermal stability from the analysis of ion-pair networks in the glutamate dehydrogenase family, *Eur. J. Biochem.* **255**, 336-346.
10. **van den Burg, B. & Eijsink, V. G.** (2002) Selection of mutations for increased protein stability, *Curr. Opin. Biotechnol.* **13**, 333-337.
11. **Eijsink, V. G., Bjork, A., Gaseidnes, S., Sirevag, R., Synstad, B., van den Burg, B. & Vriend, G.** (2004) Rational engineering of enzyme stability, *J. Biotechnol.* **113**, 105-120.
12. **Craik, D. J., Daly, N. L., Saska, I., Trabi, M. & Rosengren, K. J.** (2003) Structures of naturally occurring circular proteins from bacteria, *J. Bacteriol.* **185**, 4011-4021.
13. **Trabi, M. & Craik, D. J.** (2002) Circular proteins--no end in sight, *Trends Biochem. Sci.* **27**, 132-138.
14. **Craik, D. J., Cemazar, M., Wang, C. K. & Daly, N. L.** (2006) The cyclotide family of circular miniproteins: nature's combinatorial peptide template, *Biopolymers.* **84**, 250-66.
15. **Camarero, J. A., Fushman, D., Sato, S., Giriat, I., Cowburn, D., Raleigh, D. P. & Muir, T. W.** (2001) Rescuing a destabilized protein fold through backbone cyclization, *J. Mol. Biol.* **308**, 1045-1062.
16. **Goldenberg, D. P. & Creighton, T. E.** (1983) Circular and circularly permuted forms of bovine pancreatic trypsin inhibitor, *J. Mol. Biol.* **165**, 407-413.
17. **Iwai, H. & Pluckthun, A.** (1999) Circular beta-lactamase: stability enhancement by cyclizing the backbone, *FEBS Lett.* **459**, 166-172.
18. **Evans, T. C., Jr., Martin, D., Kolly, R., Panne, D., Sun, L., Ghosh, I., Chen, L., Benner, J., Liu, X. Q. & Xu, M. Q.** (2000) Protein trans-splicing and cyclization by a naturally split intein from the dnaE gene of *Synechocystis* species PCC6803, *J. Biol. Chem.* **275**, 9091-904.
19. **Scott, C. P., Abel-Santos, E., Wall, M., Wahnou, D. C. & Benkovic, S. J.** (1999) Production of cyclic peptides and proteins in vivo, *Proc. Natl. Acad. Sci. U S A.* **96**, 13638-13643.
20. **Iwai, H., Lingel, A. & Pluckthun, A.** (2001) Cyclic green fluorescent protein produced in vivo using an artificially split PI-PfuI intein from *Pyrococcus furiosus*, *J. Biol. Chem.* **276**, 16548-16554.
21. **Planas, A.** (2000) Bacterial 1,3-1,4-beta-glucanases: structure, function and protein engineering, *Biochim. Biophys. Acta.* **1543**, 361-382.
22. **Henrissat, B.** (1991) A classification of glycosyl hydrolases based on amino acid sequence similarities, *Biochem. J.* **280**, 309-316.
23. **Hahn, M., Olsen, O., Politz, O., Borriss, R. & Heinemann, U.** (1995) Crystal structure and site-directed mutagenesis of *Bacillus macerans* endo-1,3-1,4-beta-glucanase, *J. Biol. Chem.* **270**, 3081-308.
24. **Hahn, M., Pons, J., Planas, A., Querol, E. & Heinemann, U.** (1995) Crystal structure of *Bacillus licheniformis* 1,3-1,4-beta-D-glucan 4-glucanohydrolase at 1.8 Å resolution, *FEBS Lett.* **374**, 221-224.
25. **Keitel, T., Simon, O., Borriss, R. & Heinemann, U.** (1993) Molecular and active-site structure of a *Bacillus* 1,3-1,4-beta-glucanase, *Proc. Natl. Acad. Sci. U S A.* **90**, 5287-5291.
26. **Sambrook, J., Fritsch, E. F. & Maniatis, T.** (1989) *Molecular cloning: A laboratory Manual*, 2nd edn, Cold Spring Harbor Laboratory, Cold Spring Harbor, NY.
27. **Planas, A., Juncosa, M., Lloberas, J. & Querol, E.** (1992) Essential catalytic role of Glu134 in endo-beta-1,3-1,4-D-glucan 4- glucanohydrolase from *B. licheniformis* as determined by site-directed mutagenesis, *FEBS Lett.* **308**, 141-145.
28. **Ichiyanagi, K., Ishino, Y., Ariyoshi, M., Komori, K. & Morikawa, K.** (2000) Crystal structure of an archaeal intein-encoded homing endonuclease PI-PfuI, *J. Mol. Biol.* **300**, 889-901.
29. **Ho, S. N., Hunt, H. D., Horton, R. M., Pullen, J. K. & Pease, L. R.** (1989) Site-directed mutagenesis by overlap extension using the polymerase chain reaction, *Gene.* **77**, 51-59.
30. **Sumner, J. B. & Somers, G. F.** (1949) Dinitrosalicylic method for glucose in *Laboratory experiments in biological chemistry* (Sumner, J. B. & Somers, G. F., eds) pp. 38-39, Academic Press, New York.

31. **Gueguen, Y., Voorhorst, W. G., van der Oost, J. & de Vos, W. M.** (1997) Molecular and biochemical characterization of an endo-beta-1,3- glucanase of the hyperthermophilic archaeon *Pyrococcus furiosus*, *J. Biol. Chem.* **272**, 31258-31264.
32. **Lloberas, J., Querol, E. & Bernues, J.** (1988) Purification and Characterization of Endo-Beta-1 3-1 4-D Glucanase Activity from *Bacillus-Licheniformis*, *Applied Microbiology and Biotechnology.* **29**, 32-38.
33. **Hahn, M., Piotukh, K., Borriss, R. & Heinemann, U.** (1994) Native-like in vivo folding of a circularly permuted jellyroll protein shown by crystal structure analysis, *Proc. Natl. Acad. Sci. U S A.* **91**, 10417-10421.
34. **Ay, J., Hahn, M., Decanniere, K., Piotukh, K., Borriss, R. & Heinemann, U.** (1998) Crystal structures and properties of de novo circularly permuted 1,3-1,4-beta-glucanases, *Proteins.* **30**, 155-167.
35. **Keitel, T., Meldgaard, M. & Heinemann, U.** (1994) Cation binding to a *Bacillus* (1,3-1,4)-beta-glucanase. Geometry, affinity and effect on protein stability, *Eur. J. Biochem.* **222**, 203-214.
36. **Chiaraluce, R., Gianese, G., Angelaccio, S., Florio, R., van Lieshout, J. F., van der Oost, J. & Consalvi, V.** (2004) Calcium-induced tertiary structure modifications of endo-beta-1,3-glucanase from *Pyrococcus furiosus* in 7.9 M guanidinium chloride, *Biochem. J.* **386**, 515-524.